

1           Spatial Correlation as an Early Warning Signal of  
2           Regime Shifts in a Multiplex Disease-Behaviour  
3           Network

4           Peter C. Jentsch<sup>a,b</sup>, Madhur Anand<sup>b</sup>, Chris T. Bauch<sup>\*a</sup>

5           <sup>a</sup>*Department of Applied Mathematics, University of Waterloo, 200 University Avenue*  
6           *West, Waterloo, Ontario, Canada N2L 3G1. \*cbauch@uwaterloo.ca*

7           <sup>b</sup>*School of Environmental Sciences, University of Guelph, 50 Stone Road East, Guelph,*  
8           *Ontario, Canada N1G 2W1.*

---

9   **Abstract**

Early warning signals of sudden regime shifts are a widely studied phenomenon for their ability to quantify a system's proximity to a tipping point to a new and contrasting dynamical regime. However, this effect has been little studied in the context of the complex interactions between disease dynamics and vaccinating behaviour. Our objective was to determine whether critical slowing down (CSD) occurs in a multiplex network that captures opinion propagation on one network layer and disease spread on a second network layer. We parameterized a network simulation model to represent a hypothetical self-limiting, acute, vaccine-preventable infection with short-lived natural immunity. We tested five different network types: random, lattice, small-world, scale-free, and an empirically derived network. For the first four network types, the model exhibits a regime shift as perceived vaccine risk moves beyond a tipping point from full vaccine acceptance and disease elimination to full vaccine refusal and disease endemicity. This regime shift is preceded by an increase in the spatial correlation in non-vaccinator opinions beginning well before the bifurcation point, indicating CSD. The early warning signals occur across a wide range of parameter values. However, the more gradual transition exhibited in the empirically-derived network underscores the need for further research before it can be determined whether trends in spatial correlation in real-world social networks represent critical slowing down. The potential upside of having this monitoring ability suggests that this is a worthwhile area for further research.

10 *Keywords:* adaptive networks, multiplex networks, behavioral modelling,

11 coupled behavior-disease models, regime shifts, early warning signal

---

## 12 **1. Introduction**

13 Vaccine-preventable infectious diseases continue to impose significant bur-  
14 dens on populations around the world [1]. Access to vaccines remains a sig-  
15 nificant barrier to providing more widespread protection against infectious  
16 diseases. However, a growing obstacle to infection control is vaccine refusal,  
17 which can have a large effect on disease prevalence. For instance, the drop  
18 in vaccine coverage after Andrew Wakefield’s fraudulent 1998 paper about  
19 the mumps-measles-rubella vaccine reduced MMR coverage to as low as 61  
20 % in some areas of the United Kingdom [2]. Lower vaccine coverage caused  
21 larger measles outbreaks in the years following the publication of the Wake-  
22 field paper [3][4]. Elimination of polio in Africa was similarly interrupted  
23 when a rumor that the vaccine could cause infertility or HIV infection began  
24 spreading in 2003, when leaders of three states in north-central Nigeria boy-  
25 cotted the vaccine until it could be tested independently. The impasse was  
26 not resolved until the following year, a time period during which these states  
27 accounted for over 50% of polio cases worldwide [5, 6]. Vaccine refusal and  
28 hesitancy are also common for influenza vaccine, with non-vaccinators citing  
29 concern for side effects, lack of perception of infection risk, and doubts about  
30 vaccine efficacy as reasons to not become vaccinated [7].

31 Simple differential equation models such as the Kermack-McKendrick SIR  
32 (susceptible-infected-recovered) model published in 1927 (originally formu-  
33 lated as an integro-differential equation) [8], allow us to characterize useful  
34 measures such as the expected number of new infections caused by each in-  
35 fection, and are readily fitted to epidemiological data. Classical infection  
36 transmission models such as the Kermack-McKendrick model assume that  
37 members of the population mix homogeneously. However, in many situa-  
38 tions, infection transmission through a network—where individuals are nodes  
39 and contacts through which infection may pass are edges—are a more accu-  
40 rate description of infection dynamics [9]. Networks tend to be analytically  
41 intractable and therefore agent-based models are often used to simulate net-  
42 works. Agent-based simulations on networks allow us to specify complex in-  
43 dividual node behavior in a natural way. One of the most ambitious examples  
44 of these is the Global-Scale Agent Model, which models the daily behavior  
45 and relationships of 6.5 billion people using worldwide GIS data[10]. How-  
46 ever, agent-based network simulations have also been studied in the context

47 of nonlinear interactions between disease dynamics and individual behaviour  
48 concerning vaccines and contact avoidance [11, 12, 13, 14, 15].

49 The trajectory that an infection takes as it moves through a population is  
50 heavily influenced by the spread of health information between individuals, so  
51 more sophisticated models of disease spread often combine disease dynam-  
52 ics and social dynamics. The coupled interactions between individual be-  
53 haviour and disease dynamics have been modelled under various frameworks  
54 and placed under various rubrics including: epidemic games [16], coupled  
55 behaviour-disease models [12, 17, 18], socio-epidemiology, economic epidemi-  
56 ology and behavioural modeling [19]. . A more recent trend in epidemio-  
57 logical modeling is to abstract these two subsystems into (1) an information  
58 transfer network through which information flows between individuals, and  
59 (2) a separate physical disease transmission network. A system where each  
60 node is part of two or more different networks is called a multiplex net-  
61 work, and is a natural way to implement a coupled disease-behaviour system  
62 [20, 18]. For instance, the simultaneous spread of disease and disease aware-  
63 ness over adaptive multiplex networks with scale-free degree distributions  
64 has been studied [21]. Similarly, a three layer network to model the diffusion  
65 of infection, awareness, and preventative measures along different contact  
66 networks was found to reasonably approximate empirical influenza data[22].  
67 Similar approaches consider coupled human and ecological dynamics, which  
68 present the opposite problem of species that humans wish to preserve instead  
69 of eradicate [23, 24, 25, 26].

70 The nonlinear coupling between disease and social processes creates feed-  
71 back loops between infection prevention mechanisms and disease spread.  
72 Nonlinear feedback in other complex systems such as from solid state physics  
73 and theoretical socio-ecology has often been shown to yield critical transitions  
74 [27, 28, 26]. A critical transition is defined as an abrupt shift from an exist-  
75 ing dynamical regime to a strongly contrasting (and sometimes unfavourable)  
76 dynamical regime as some external parameter is pushed past a bifurcation  
77 point [29, 30]. Fortunately, critical transitions (and other regime shifts as-  
78 sociated with a bifurcation where the dominant eigenvalue of the Jacobian  
79 matrix around the equilibrium approaches zero) often exhibit characteris-  
80 tic early warning signals beforehand that allow these shifts to be predicted  
81 [31, 32, 30]. Critical slowing-down (CSD) based indicators were one of the  
82 first early warning signals to be studied. CSD occurs because the speed with  
83 which a system responds to perturbations slows as it approaches bifurcations  
84 where the magnitude of the dominant eigenvalue of the Jacobian approaches

85 zero at the bifurcation point. Since nearly all systems in the real world are  
86 subject to perturbations, the lag-1 autocorrelation of a time series can be  
87 used as a relatively universal (or at least potentially common) indicator of  
88 CSD. Lag-1 autocorrelation appears to be a robust statistic and has been  
89 shown to be present in predicting catastrophic bifurcations in complex real  
90 world systems such as the global climate[33], human nervous systems[34],  
91 and stock markets[35].

92 The discrete fourier transform (DFT) of a network is another example  
93 of a CSD-based early warning signal. Under some assumptions, the Weiner-  
94 Kinchin Theorem shows that we can use the discrete Fourier transform (DFT)  
95 to measure spatial correlation in system state, and this has been shown to  
96 work in some ecological applications [36] [37]. Lag-1 spatial correlation can in  
97 some cases provide a better early warning signal than time-domain methods,  
98 because "a spatial pattern contains much more information than does a single  
99 point in a time series, in principle allowing shorter lead times" before the  
100 critical transition occurs [38, 31]. This observation has been corroborated in  
101 three ecological dynamical systems[31].

102 Early warning signals of regime shifts in coupled behaviour-disease net-  
103 works have received relatively little attention in the literature on modelling  
104 interactions between disease dynamics and human behaviour. This appears  
105 to be a significant knowledge gap because early warning signals for vaccine  
106 scares could help public health anticipate widespread vaccine refusal and  
107 prepare for outbreak response in advance, as well as build efforts to improve  
108 trust between the public and the health authorities. In this paper we use an  
109 agent-based model on a two-layer multiplex network to simulate the coupled  
110 disease dynamics of a vaccine-preventable infection and social dynamics of  
111 vaccination in a population. We show that spatial correlation can be used as  
112 an early warning signal for regime shifts in this system on most (but not all)  
113 network topologies. In the next section we discuss the model structure and  
114 methods of analysis, followed by a section on results and finally a discussion  
115 section.

## 116 **2. Methods**

### 117 *2.1. Simulation*

118 Our agent-based model simulated a population of 10,000 individuals (nodes),  
119 where every node belongs to two different connectivity networks: a transmis-  
120 sion network and a social network. In the transmission network, each node

121 is connected to other nodes from which they can contract infection. Two  
 122 nodes are linked in the social network if they can be influenced by one an-  
 123 other’s opinions on vaccination. These networks were simulated as fixed  
 124 graphs upon which stochastic processes occurred, with a variety of degree  
 125 distributions and average path lengths.

126 We modelled a hypothetical acute, self-limiting infection with rapidly  
 127 waning natural immunity Each node on the physical layer is in one of four  
 128 possible states: susceptible ( $S$ ), infected ( $I$ ), recovered ( $R$ ), or vaccinated  
 129 ( $V$ ). Each node on the social layer also has an opinion on the vaccine: they  
 130 are either a non-vaccinator ( $\eta$ ), or a vaccinator( $\nu$ ). We will denote the the  
 131 biological state of a node  $v$  by  $B(v)$ , and the opinion of a node  $v$  by  $\Theta(v)$ .  
 132 The transmission network is a graph denoted by  $T(V, E_T)$ , and the social  
 133 network is a graph denoted by  $O(V, E_O)$ . We assume that they share the  
 134 same set of vertices  $V$  although this assumption could be relaxed in future  
 135 work. The set of nodes in the neighbourhood of  $v$  is  $adj_T(v)$  or  $adj_O(v)$  for  
 136 the transmission and the social network respectively.

137 The algorithm used to simulate the social and transmission processes used  
 138 discrete timesteps. At each time step, for each  $v \in V$ :

- 139 • If  $B(v) = I$ , then for all  $u \in adj_T(v)$  such that  $B(u) = S$  and  $\Theta(u) \neq \nu$ ,  
 140 set  $B(u) = I$  with probability  $p$  (infection event)
- 141 • If  $B(v) = I$ , let  $B(v) = R$  with probability  $r$  (natural recovery event)
- 142 • If  $B(v) = R$ , set  $B(v) = S$  with probability  $\gamma$  (loss of immunity event)
- 143 • If  $B(v) = S$ , set  $B(v) = I$  with probability  $\sigma \ll 1$  (case importation  
 144 event)
- 145 • Choose some node  $u \in adj_O(v)$  uniformly at random. If  $\Theta(v) \neq \Theta(u)$ ,  
 146 then  $P(\eta \rightarrow \nu) = \Phi(E_V - E_N)$ , and  $P(\nu \rightarrow \eta) = 1 - \Phi(E_V - E_N)$   
 147 where

$$E_V = -c_v + c_n, \tag{1}$$

$$E_N = -c_I \mathfrak{J}(v), \tag{2}$$

149 where  $\Phi$  is a sigmoid function such that  $\Phi(\infty) = 1$ ,  $\Phi(-\infty) = 0$ ,  
 150  $\Phi(0) = 0.5$  as described in previous models (opinion change event)  
 151 [39]. In our implementation,  $\Phi(x) = \frac{1}{1+e^{-\beta x}}$ ,  $c_v$  is the perceived cost of

152 vaccination (due to infection risks),  $c_I$  is the perceived cost of infection  
153 (due to infection risks),  $\beta$  controls the steepness of the sigmoid function,  
154 and  $\mathfrak{J}(v) = |\{u \in \text{adj}_T(v) : B(u) = I\}|$  is the number of infected nodes  
155 adjacent to  $v$  in the transmission network.  $c_n$  represents some outside  
156 incentive that a person might have for vaccinating, such as peer ap-  
157 proval, school admission requirements, or tax incentives. Normalizing  
158 both payoff equations by  $c_I$  yields

$$E_V = -c + \xi \quad (3)$$

159

$$E_N = -\mathfrak{J}(v) \quad (4)$$

160 where  $c$  is the ratio of perceived vaccine risk to perceived disease risk,  
161 and  $\xi = \frac{c_n}{c_I}$  is the ratio of the vaccination incentive to the perceived  
162 disease risk. Since changes in perceived vaccine risk are controlled  
163 through changes in  $c$ , we will vary  $c$  in our analysis. We assume the  
164 vaccine is perfectly efficacious.

- 165 • With probability  $\epsilon$ ,  $v$  changes opinions (random opinion change event).  
166 That is, if  $\Theta(v) = \nu$ , set  $\Theta(v) = \eta$  and vice-versa.
- 167 • If the opinion of a node changes to vaccinator, then their physical state  
168 changes to immunized immediately. If they change back to a non-  
169 vaccinator, they become susceptible immediately.

170 We applied synchronized updating to the network: the change in state re-  
171 sulting from each rule is stored and applied after every rule is checked, so  
172 the order of the above steps does not matter.

173 The result of these rules is a feedback loop where, depending on the rel-  
174 ative costs of vaccination and infection, the population tends not to exhibit  
175 a mixture of strategies except near the critical values of  $c$ . When  $c < \xi$ , the  
176 payoff to vaccinate  $E_V$  is positive and thus exceeds the payoff not to vacci-  
177 nate  $E_N$  which always obeys  $E_N \leq 0$ . In this case, in the limit as  $\beta \rightarrow \infty$ , all  
178 nodes are therefore vaccinators and the infection dies out. However, when  
179  $c > \xi$  and thus  $E_V < 0$ , the disease-free equilibrium destabilizes since  $E_N \approx 0$   
180 in the absence of sustained transmission. In general, since the vast major-  
181 ity of nodes do not have infected neighbours at the disease-free equilibrium,  
182 there is a rapid shift in the population to non-vaccinator opinions as well  
183 as epidemic outbreaks. For larger values of  $\beta$ , the function controlling the  
184 opinion-switching as a function of the payoff difference between vaccinator

185 and non-vaccinator strategies is steeper, and the population transition from  
186 non-vaccinator to vaccinator strategies is therefore sharper, yielding a crit-  
187 ical transition. However, we will use the more general term ‘regime shift’  
188 throughout this paper, since the transition can be made more or less abrupt  
189 by changing the value of  $\beta$ .

## 190 2.2. Early Warning Signal Analysis

191 As the system approaches a regime shift, the dominant eigenvalue of  
192 the underlying dynamical system will approach zero. Therefore, it will take  
193 longer for the system to recover from perturbations to the steady state. In  
194 a spatially extended population, this will increase population heterogeneity  
195 as small clusters of non-vaccinators begin to emerge, as well as causing long-  
196 range correlations to develop across the network in a detectable way [31].  
197 This development is reflected by an increase in a statistic called the lag-1  
198 spatial correlation (lag-1 SC). We used Moran’s I to measure the lag-1 SC  
199 of non-vaccinators as described in [40]. Moran’s I is widely used to calculate  
200 the spatial correlation for early warning signals [41, 42, 43].

201 Let  $G = (V, E)$  be a graph with  $n$  nodes,  $adj(v)$  be the set of vertices  
202 adjacent to  $v$ , and  $f(v)$  be a binary function such that  $f(v) = 1$  if  $v$  is a  
203 vaccinator, and  $f(v) = 0$  otherwise. We define Moran’s I at lag-1, called  $M$   
204 to prevent confusion with the Infected state, as:

$$M = \frac{\sum_{v \in V} I_v}{|E|} \quad (5)$$

$$M_v = \frac{n(f(v) - \bar{x}) \sum_{w \in adj(v)} (f(w) - \bar{x})}{\sum_{w \in V} (f(w) - \bar{x})^2} \quad (6)$$

205 where  $\bar{x} = \frac{1}{n} \sum_{v \in V} f(v)$  is the fraction of vaccinators in the network. Far  
206 from the regime shift, we have that  $\bar{x} \approx 1$  and  $f \approx 1$  for all nodes, thus  
207  $I \approx 0$ . However, as resilience to perturbations declines close to the regime  
208 shift, the population become more heterogeneous. This causes  $f - \bar{x} \approx -1$   
209 in correlated non-vaccinator clusters, thus  $I$  increases.

210 For each realization, the simulation was run long enough for the spatial  
211 correlation to stabilize (3500 timesteps), and the equilibrium value was cal-  
212 culated as the average of the next 500 measurements. The equilibrium lag-1  
213 SC was obtained for 100 realizations of the simulation, and these values were  
214 averaged to obtain a data point for every value of  $c$ . The social network  
215 and the transmission network are always both the same type of network, but  
216 independently generated.



Parameter	Value	Definition
$p$	0.5	Probability that an infected node infects a given susceptible neighbour
$r$	0.07143	Probability that an infected node recovers
$\gamma$	0.001369	Probability that a recovered node becomes susceptible
$\epsilon$	0.001369	Probability that a node randomly switches their opinion on vaccination
$\sigma$	0.016666	Probability of disease reintroduction
$\xi$	0	Parameter governing incentive to become vaccinated
$c$	0.1	Ratio of perceived risk of vaccine to perceived risk of disease
$\beta$	1	Parameter controlling the steepness of $\Phi$

Table 1: Parameter definitions and baseline parameter values in probability per timestep (unless otherwise stated). One timestep was interpreted to correspond to one day.

### 217 2.3. Parameter Values

218 Baseline parameter values appear in Table 1. The parameter values were  
219 chosen to qualitatively represent a hypothetical acute-self limiting infection  
220 with waning natural immunity, such as the case of meningococcal infection,  
221 influenza or pertussis [44, 45, 46, 47]. The value for  $r$  corresponds to a mean  
222 duration of infection of 14 days, the value for  $\gamma$  corresponds to losing nat-  
223 ural immunity after two years, and the value for  $\sigma$  corresponds to a case  
224 importation event in the network once every two months. We conduct uni-  
225 variate sensitivity analysis with respect to  $r$  and  $\sigma$ , since they are important  
226 parameters governing the natural history of the infection. For the baseline  
227 parameter values,  $\xi$  is set to zero without loss of generality. The value of  
228  $c$  will be varied in the analysis of early warning signals.  $\epsilon > 0$  is required  
229 to prevent the population from fixating on one of the two strategies. To  
230 initialize each stochastic realization, one randomly chosen node is infected,  
231 and each node is a vaccinator with probability 0.5.

### 232 2.4. Networks

233 We ran our model on five different networks: Erdos-Renyi [48], Barabasi-  
234 Albert [49], square lattice (or grid), Kleinberg small world[50], and ten sub-  
235 sets of a network constructed by the Network Dynamics and Simulation and



236 Science Laboratory (NDSSL), based on GIS data from the city of Portland  
237 [51].

238 An Erdos-Renyi network is simply given a set of nodes  $V$  and  $v, w \in V$ ,  
239  $v$  is connected to  $w$  with some probability  $p$ . In our Erdos-Renyi network  
240 model, we used a connection probability of 0.001, so each node has degree  
241 10 on average.

242 The Barabasi-Albert model yields networks with a scale-free (or power-  
243 law) node degree distribution. Starting with a small initial connected network  
244  $(V, E)$ , new nodes are added to  $V$  one at a time. Where the probability that  
245 the new node is connected to an existing node  $v \in V$  is  $p_v = \frac{\text{deg}(v)}{\sum_{w \in V} \text{deg}(w)}$ . To  
246 ensure that the network is always connected, new nodes are also connected  
247 to  $m$  existing vertices, chosen uniformly at random. The Barabasi-Albert  
248 networks we used had  $m = 1$ .

249 Our lattice with  $n = 10,000$  nodes was built as follows: if the nodes  
250 are arranged on the integer points of a square  $\sqrt{n}$  units wide, each node is  
251 connected to the nodes within a unit distance up or down (but not both).  
252 Because lattice networks are not random, there is no difference between the  
253 social and transmission networks and therefore this is effectively not a mul-  
254 tiplex network.

255 The Kleinberg small world network is defined as a square lattice, where  
256 additional edges are added between some nodes  $v$  and  $w$  with a probability  
257 proportional to  $1/d(v, w)$ . The result of this process is a network with a very  
258 short average path length. In our implementation, nodes only gain extra  
259 edges with 0.1 probability.

260 The empirically-derived networks from the NDSSL dataset are designed to  
261 have some of the properties of a real contact network, being derived from the  
262 population of Portland, Oregon. We used a set of ten subnetworks sampled  
263 from the NDSSL dataset and constructed in such a way to share the same  
264 properties as the original dataset (see Ref. [39] and supplementary appendix  
265 for details). The subnetworks had an average path length of  $4.020 \pm 0.126$ ,  
266 and an average clustering coefficient of  $0.747 \pm 0.006$ . For each run, two  
267 networks were chosen from the 10 networks uniformly at random and one  
268 was set as the social network, with the other as the transmission network.

## 269 **3. Results**

### 270 *3.1. Model dynamics*

271 We generated time series of the percentage of vaccinators and percent-  
272 age of infected persons for each of the networks, in order to illustrate the  
273 basic dynamics exhibited by the model. We used baseline parameter values  
274 everywhere (Table 1) except that  $c = 0.3$ . For all networks we initialized  
275 the population to have a low initial number of vaccinators and a large initial  
276 number of susceptible persons. These initial conditions caused the incidence  
277 of infection to skyrocket at the beginning of the simulation for all network  
278 types (Figure 1). Immediately after this initial outbreak, susceptible neigh-  
279 bours of infected persons get vaccinated, thereby reducing prevalence.

280 After this initial spike, the dynamics settle down into pseudo-stable pat-  
281 terns that vary widely depending on network type. More frequent outbreaks  
282 appear to occur on networks with higher degree, which is consistent with intu-  
283 ition (Figure 1). The random network exhibits relatively regular outbreaks  
284 (Figure 1a), while the square lattice, Barabasi-Albert network, and small  
285 world network exhibit more irregular dynamics consisting of large outbreaks  
286 interspersed with periods of very low vaccine coverage and infection preva-  
287 lence (Figure 1b-d). However, during certain phases in the time series, the  
288 small-world network appears to transition to a regime of sustained endemic  
289 infection similar to that observed for the random network (Figure 1d). The  
290 empirically-derived network exhibits small stochastic fluctuations around an  
291 equilibrium, and the percentage of vaccinators is significantly higher in the  
292 empirically-derived network than in the other four networks (Figure 1e).

### 293 *3.2. Regime shifts*

294 We carried out this simulation experiment for a range of values of  $c$  to  
295 understand how dynamics respond to changes in the perceived vaccine risk  
296  $c$ . We computed the long-term average prevalence of infected persons and  
297 vaccinators for each value of  $c$  tested. As  $c$  approaches zero from below (for  
298  $\xi = 0$ ), a transition from a regime of high vaccine coverage and low infection  
299 prevalence to a regime of low vaccine coverage and endemic infection should  
300 be observed, since for  $c > 0$ , the payoff to vaccinate becomes less than the  
301 payoff not to vaccinate.

302 In the simulations we observe a transition in the percentage of non-  
303 vaccinators as a function of the perceived vaccine risk  $c$  in most of the network  
304 types (Figure 2). As  $c$  approaches zero, the prevalence of vaccinators declines

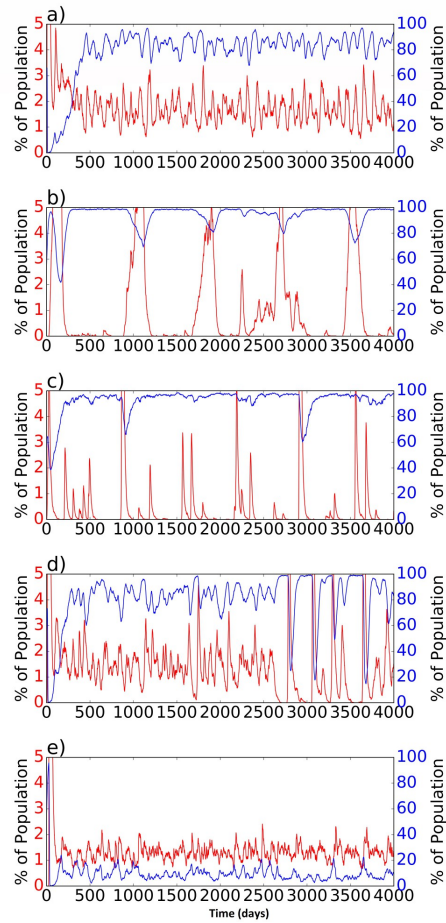


Figure 1: Time series for a typical simulation on each network type: a) random network, b) square lattice, c) Barabasi-Albert network, d) Small world network, e) empirically-derived networks. Red line is percentage of infected individuals in the population; blue line is percentage of vaccinators in the population. Parameter values are as in Table 1 except  $c = 0.3$ .

305 dramatically in the first four networks. The transition appears gradual (non-  
306 critical) in the empirically-derived network (Figure 2e). We speculate this  
307 is due to the greater heterogeneity exhibited by the empirically-derived net-  
308 work than the other four idealized network types. The percentage of infected  
309 persons in each network shows similar transitions, even in the latter network  
310 (Figure 2e). We also note that the transition is sharper when the sigmoid  
311 function used in decision-making is steeper (higher  $\beta$ ; results not shown).

### 312 3.3. *Early warning signals*

313 Indicators such as spatial correlation can signal an impending critical  
314 transition in spatially structured ecological systems [31]. Although theo-  
315 retical results are not available for coupled behaviour-disease dynamics on  
316 multiplex networks, the universality of dynamics near local bifurcations of  
317 dynamical systems [32] suggests that similar early warning signals should be  
318 observed in our system.

319 In spatially extended critical phenomena, the plot of spatial correlation  
320 versus a bifurcation parameter such as  $c$  is linear on a log-linear plot [52].  
321 Hence, we computed the average lag-1 spatial correlation (SC) across the  
322 entire time series. We repeated this for many values of  $c$  and plotted lag-1  
323 AC versus  $c$  on a log-linear scale. As noted previously, we expect near the  
324 threshold  $c = 0$  where the costs and benefits of the vaccine become balanced,  
325 that critical slowing down should emerge in the network, and that this should  
326 manifest as increased spatial correlation. As we increase  $c$  from negative to  
327 positive, small clusters of non-vaccinators begin to appear. Each day every  
328 node samples a random neighbour, and the only other way for that node to  
329 switch opinions is if the randomly sampled neighbour has a different opinion  
330 that they do (see Methods). As a result, we expect to see clusters of non-  
331 vaccinators emerge, which causes the lag-1 SC to increase before the critical  
332 transition (and after which almost everyone because a non-vaccinator) (figure  
333 3).

334 This pattern is observed in simulations for all network types. As the  
335 regime shift at  $c = 0$  is approached from negative values of  $c$  (corresponding  
336 to a rise in perceived vaccine risks), we observe a clear and linear increase  
337 in the time-averaged lag-1 SC, in plots of the natural logarithm of lag-1 SC  
338 versus  $c$  (Figure 4). This is robust to values of the disease transmission  
339 probability,  $p$  (Figure 4).

340 However, there is a notable difference in y-axis scales for the random and  
341 small-world networks (Figure 4a,d). Overall these networks show a smaller

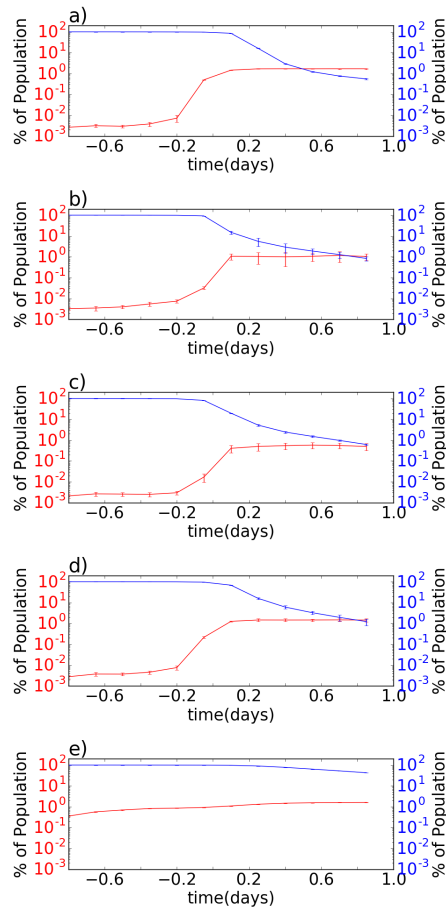


Figure 2: The time-averaged percentage of infected persons and vaccinators as a function of relative vaccine cost  $c$ , showing a critical transition near  $c = 0$  on the a) random network, b) square lattice, c) Barabasi-Albert network, d) Small world network, and a more gradual transition on the e) empirically-derived networks. All parameters are as in Table 1 except for  $c$ , which is being varied. The blue line represents the percentage of vaccinators, and the red line percentage of infected. Error bars represent the standard deviation over the 100 realizations.

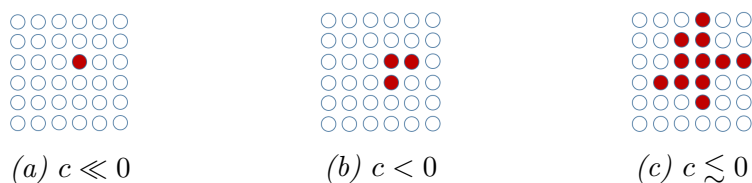


Figure 3: Visualization of non-vaccinator spatial correlation on a square lattice. As  $c$  approaches the critical transition at  $c = 0$ , clusters of non-vaccinators (red) begin to appear, increasing the spatial correlation of non-vaccinators.

342 increase in spatial correlation, possibly due to the smaller average path length  
343 in these networks. Furthermore, lag-1 SC in the empirically-derived network  
344 has a nonlinear and more gradual response to changes in  $c$ , which matches the  
345 lack of a sharp critical transition in that network. Sensitivity analyses over  
346  $r$  and  $\sigma$  confirm the same patterns, except in the extreme case of  $r = 0.02$   
347 where infected individuals never recover (Figure 5).

348 We observe that the rise in the natural logarithm of lag-1 SC begins well  
349 before the number of non-vaccinators begins to increase appreciably (com-  
350 pare  $c \in [-0.8, -0.2]$  in Figure 4 versus Figure 2). Therefore, tracking lag-1  
351 SC can provide an early warning signals of potential shifts in population vac-  
352 cinating behaviour that would not be accessible simply by extrapolating the  
353 number of non-vaccinators using a linear regression, for instance. Moreover,  
354 this rise in lag-1 SC is highly robust to network type and parameter value,  
355 due to the fundamental assumption that a node's vaccination status is influ-  
356 enced by the opinions of the nodes in their social neighbourhood. However,  
357 the location of the regime shift in  $c$  is related to the average node degree:  
358 with an average node degree of 100, the regime shift occurs at approximately  
359  $c = 2.4$ .

#### 360 4. Discussion

361 Here we studied regime shifts in coupled behaviour-disease dynamics on  
362 a multiplex network where an infectious disease is transmitted through the  
363 physical network layer, and the social layer describes a population where  
364 everyone has either a pro-vaccine or an anti-vaccine opinion. These simu-  
365 lation results show the presence of critical slowing down near a bifurcation  
366 in the multiplex network corresponding to a switch from predominant vac-  
367 cinating behaviour and disease elimination, to predominant non-vaccinating

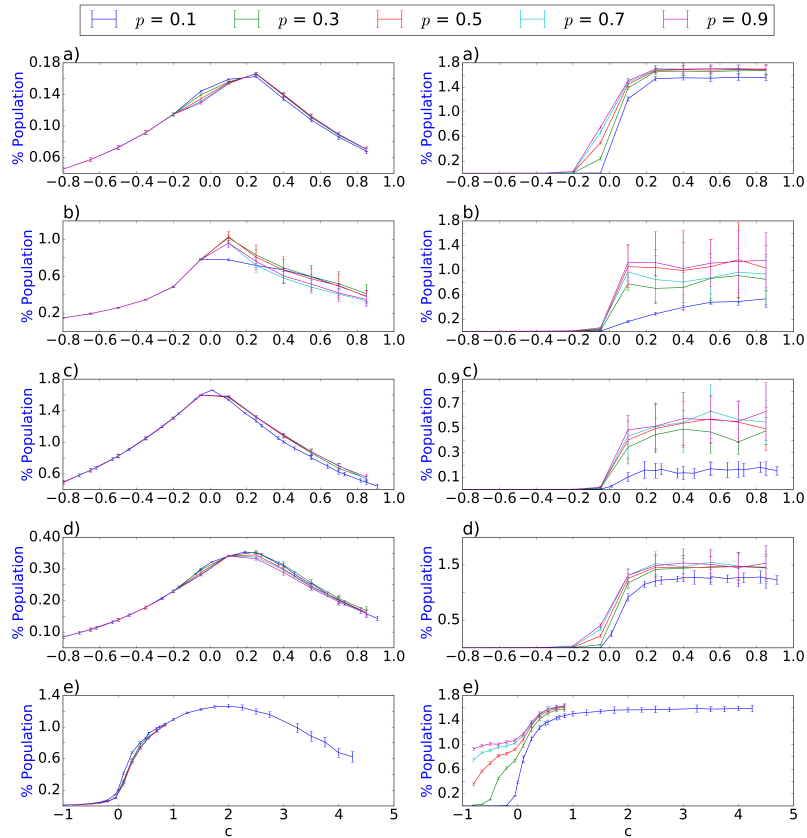


Figure 4: The natural logarithm of the time-averaged lag-1 SC of nonvaccinators, and the percentage of infected nodes, for a range of values of  $c$ , showing a linear increase in lag-1 SC in a log-linear plot as the critical transition is approached on a) random network, b) square lattice, c) Barabasi-Albert network, d) Small world network, e) empirically-derived networks. All other parameter values are as in Table 1.



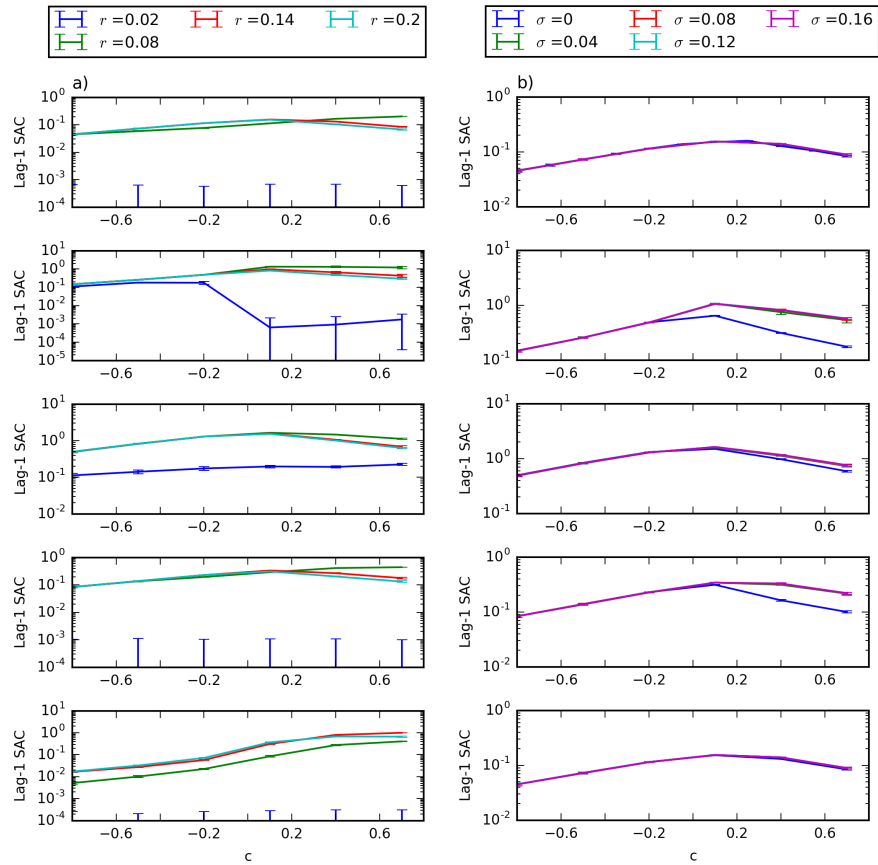


Figure 5: The natural logarithm of the time-averaged lag-1 SC of nonvaccinators for a range of values of  $c$  at selected values of a)  $r$  and b)  $\sigma$ , showing a linear increase in lag-1 SC in a log-linear plot as the critical transition is approached. Networks types from top row to bottom row are: random network, square lattice, Barabasi-Albert network, small world network, and empirically-derived networks. All parameters besides  $r$ ,  $\sigma$  and  $c$  are the same as Table 1.

368 behaviour and disease endemicity. Critical slowing down was clearly man-  
369 ifested in all network types and across a broad range of parameter values,  
370 with the exception of the empirically derived network. This exception may  
371 have been on account of the greater heterogeneity of the network structure  
372 causing lack of a sharp transition to non-vaccinating behaviour.

373 Hence, the results suggest that it may be possible to use lag-1 spatial cor-  
374 relation in social networks as an early warning signal of widespread vaccine  
375 refusal in a population. However, the lack of a clear transition in the case of  
376 the network that was empirically derived (from NDSSL data) suggests that  
377 further research must be conducted in order to determine how and whether  
378 it would be possible to detect such early warning signals in real-world social  
379 networks, and what the trends in correlation indicators might signify. We  
380 speculate that our approach might have failed for the empirical network due  
381 to multiple sources of heterogeneity in network structure such as: a highly  
382 dispersed node degree distribution; the presence of disconnected subgraphs;  
383 and/or differing network structure in different parts of the network. How-  
384 ever, it is possible that including peer pressure (social norms) in the model  
385 might cause population opinion states to shift to bistable boundary equilibria  
386 corresponding to all-vaccinator or no-vaccinator population compositions—as  
387 has been observed in other socio-ecological models—and thus restore the fea-  
388 sibility of early warning signals [26]. Our model also assumed that networks  
389 are static and that the two layers are perfectly correlated. Neither condition  
390 holds in real populations, and these simplifying assumptions could be relaxed  
391 in future work.

392 It is also possible to tailor this model to specific infectious diseases such as  
393 measles or influenza by modifying the model to include relevant vital dynam-  
394 ics, disease natural history, and vaccine characteristics. This is particularly  
395 important since disease natural history can have a significant impact on dis-  
396 ease dynamics [44, 53], and vaccine coverage can vary widely between both  
397 vaccines and populations [54, 55]. Further to this point, there are indica-  
398 tions that some disease dynamics, such as meningococcal disease, are in a  
399 state of self-evolved criticality in their naturally circulating dynamics (i.e.  
400 always close to a critical point) [56]. The impact of ever-present critical dis-  
401 ease dynamics on the detectability of early warning signals of a regime shift  
402 in a socio-epidemiological state require further research. For instance, the  
403 critical disease dynamics could serve to mask early warning signals of socio-  
404 epidemiological regime shifts. This would motivate a search for indicators  
405 that can distinguish the socio-epidemiological signal from the background of

406 critical disease dynamics.

407 Finally, future research could seek early warnings signals in lag-1 SC  
408 measurements from social networks derived from social media data sources  
409 such as Twitter. Lag-1 SC is readily calculated if the sentiment of Twitter  
410 users toward vaccines can be assessed as pro- or anti-vaccine. However, the  
411 Twitter follower network is a directed graph that changes in time, therefore  
412 additional theoretical refinements are necessary. Moreover, our method as-  
413 sumes perfect knowledge of the state of nodes on the social layer, whereas in  
414 reality this information is partial. Future work should also explore whether  
415 censored data on vaccine opinions changes the reliability of the early warning  
416 indicators we explored in this paper. This could be addressed by extended  
417 models with a parameter for censoring and a distinction between actual and  
418 observed opinion status.

419 Lag-1 spatial correlation appears to be a robust early warning signal for  
420 predicting regime shifts in vaccine uptake under the conditions we studied,  
421 indicating potential for worthwhile additional study in the context of coupled  
422 behaviour-disease interactions.

## 423 5. Acknowledgments

424 The authors are grateful for helpful comments from the editor and reviewers.  
425 This research was funded by Natural Sciences and Engineering Research  
426 Council of Canada (NSERC) Discovery Grants to MA and CTB.

## 427 6. References

- 428 [1] A. D. Lopez and C. D. Mathers, “Measuring the global burden of dis-  
429 ease and epidemiological transitions: 2002–2030,” *Annals of tropical*  
430 *medicine and parasitology*, 2013.
- 431 [2] S. Murch, “Separating inflammation from speculation in autism,” *The*  
432 *Lancet*, vol. 362, pp. 1498–1499, 2003.
- 433 [3] M. Alazraki, “The autism vaccine fraud: Dr. wakefield’s costly lie to  
434 society,” Dec 2011.
- 435 [4] V. A. Jansen, N. Stollenwerk, H. J. Jensen, M. Ramsay, W. Edmunds,  
436 and C. Rhodes, “Measles outbreaks in a population with declining vac-  
437 cine uptake,” *Science*, vol. 301, no. 5634, pp. 804–804, 2003.

- 438 [5] C. Chen, “Rebellion against the polio vaccine in nigeria: implications  
439 for humanitarian policy,” *African Health Sciences*, vol. 4, pp. 205–207,  
440 2004.
- 441 [6] A. S. Jegede, “What led to the Nigerian boycott of the polio vaccination  
442 campaign?,” *PLoS Med*, vol. 4, 2007.
- 443 [7] N. H. Fiebach and C. M. Viscoli, “Patient acceptance of influenza vacci-  
444 nation,” *The American journal of medicine*, vol. 91, no. 4, pp. 393–400,  
445 1991.
- 446 [8] W. O. Kermack and A. G. McKendrick, “A contribution to the mathe-  
447 matical theory of epidemics,” *Proceedings of the Royal Society of London*  
448 *A: Mathematical, Physical and Engineering Sciences*, vol. 115, no. 772,  
449 pp. 700–721, 1927.
- 450 [9] S. Bansal, B. T. Grenfell, and L. A. Meyers, “When individual behaviour  
451 matters: homogeneous and network models in epidemiology,” *Journal*  
452 *of the Royal Society Interface*, vol. 4, no. 16, pp. 879–891, 2007.
- 453 [10] J. Parker and J. M. Epstein, “A distributed platform for global-scale  
454 agent-based models of disease transmission,” *ACM Transactions on*  
455 *Modeling and Computer Simulation*, vol. 22, no. 1, pp. 1–25, 2011.
- 456 [11] L. B. Shaw and I. B. Schwartz, “Fluctuating epidemics on adaptive  
457 networks,” *Physical Review E*, vol. 77, no. 6, p. 066101, 2008.
- 458 [12] A. Perisic and C. T. Bauch, “Social contact networks and disease  
459 eradicability under voluntary vaccination,” *PLoS Comput Biol*, vol. 5,  
460 p. e1000280, 02 2009.
- 461 [13] F. Fu, D. I. Rosenbloom, L. Wang, and M. A. Nowak, “Imitation dy-  
462 namics of vaccination behaviour on social networks,” *Proceedings of*  
463 *the Royal Society of London B: Biological Sciences*, vol. 278, no. 1702,  
464 pp. 42–49, 2011.
- 465 [14] S. Funk, E. Gilad, C. Watkins, and V. A. Jansen, “The spread of aware-  
466 ness and its impact on epidemic outbreaks,” *Proceedings of the National*  
467 *Academy of Sciences*, vol. 106, no. 16, pp. 6872–6877, 2009.

- 468 [15] H.-F. Zhang, Z.-X. Wu, M. Tang, and Y.-C. Lai, “Effects of behav-  
469 ioral response and vaccination policy on epidemic spreading-an approach  
470 based on evolutionary-game dynamics,” *Scientific reports*, vol. 4, 2014.
- 471 [16] W.-X. Wang, Y.-C. Lai, and C. Grebogi, “Effect of epidemic spreading  
472 on species coexistence in spatial rock-paper-scissors games,” *Phys. Rev.  
473 E*, vol. 81, p. 046113, Apr 2010.
- 474 [17] A. Perisic and C. T. Bauch, “A simulation analysis to characterize the  
475 dynamics of vaccinating behaviour on contact networks,” *BMC Infec-  
476 tious Diseases*, vol. 9, no. 1, p. 1, 2009.
- 477 [18] Z. Wang, M. A. Andrews, Z.-X. Wu, L. Wang, and C. T. Bauch,  
478 “Coupled disease-behavior dynamics on complex networks: A review,”  
479 *Physics of Life Reviews*, vol. 15, pp. 1–29, 2015.
- 480 [19] E. P. Fenichel, C. Castillo-Chavez, M. G. Ceddia, G. Chowell, P. A. G.  
481 Parra, G. J. Hickling, G. Holloway, R. Horan, B. Morin, C. Perrings,  
482 and et al., “Adaptive human behavior in epidemiological models,” *Pro-  
483 ceedings of the National Academy of Sciences*, vol. 108, pp. 6306–6311,  
484 Apr 2011.
- 485 [20] C. T. Bauch and A. P. Galvani, “Social factors in epidemiology,” *Science*,  
486 vol. 342, no. 6154, pp. 47–49, 2013.
- 487 [21] C. Granell, S. Gómez, and A. Arenas, “Dynamical interplay between  
488 awareness and epidemic spreading in multiplex networks,” *Phys. Rev.  
489 Lett.*, vol. 111, p. 128701, Sep 2013.
- 490 [22] L. Mao and Y. Yang, “Coupling infectious diseases, human preventive  
491 behavior, and networks - a conceptual framework for epidemic model-  
492 ing,” *Social Science and Medicine*, vol. 74, pp. 167–175.
- 493 [23] C. Innes, M. Anand, and C. T. Bauch, “The impact of human-  
494 environment interactions on the stability of forest-grassland mosaic  
495 ecosystems,” *Scientific reports*, vol. 3, p. 2689, 2013.
- 496 [24] L.-A. Barlow, J. Cecile, C. T. Bauch, and M. Anand, “Modelling in-  
497 teractions between forest pest invasions and human decisions regarding  
498 firewood transport restrictions,” *PLoS One*, vol. 9, no. 4, p. e90511,  
499 2014.

- 500 [25] K. A. Henderson, C. T. Bauch, and M. Anand, “Alternative stable states  
501 and the sustainability of forests, grasslands, and agriculture,” *Proceed-*  
502 *ings of the National Academy of Sciences*, vol. 113, no. 51, pp. 14552–  
503 14559, 2016.
- 504 [26] R. P. Sigdel, M. Anand, and C. T. Bauch, “Competition between in-  
505 junctive social norms and conservation priorities gives rise to complex  
506 dynamics in a model of forest growth and opinion dynamics,” *Journal*  
507 *of theoretical biology*, vol. 432, pp. 132–140, 2017.
- 508 [27] Q. Guo, X. Jiang, Y. Lei, M. Li, Y. Ma, and Z. Zheng, “Two-stage ef-  
509 fects of awareness cascade on epidemic spreading in multiplex networks,”  
510 *Phys. Rev. E*, vol. 91, p. 012822, Jan 2015.
- 511 [28] S. Xia and J. Liu, “A computational approach to characterizing the  
512 impact of social influence on individuals vaccination decision making,”  
513 *PLoS ONE*, vol. 8, p. e60373, 04 2013.
- 514 [29] M. Scheffer, J. Bascompte, W. A. Brock, V. Brovkin, S. R. Carpenter,  
515 V. Dakos, H. Held, E. H. V. Nes, M. Rietkerk, and G. Sugihara, “Early-  
516 warning signals for critical transitions,” *Nature*, vol. 461, pp. 53–59,  
517 2009.
- 518 [30] C. T. Bauch, R. Sigdel, J. Pharaon, and M. Anand, “Early warning  
519 signals of regime shifts in coupled human–environment systems,” *Pro-*  
520 *ceedings of the National Academy of Sciences*, p. 201604978, 2016.
- 521 [31] V. Dakos, E. van Nes, R. Donangelo, H. Fort, and M. Scheffer, “Spa-  
522 tial correlation as leading indicator of catastrophic shifts,” *Theoretical*  
523 *Ecology*, vol. 3, no. 3, pp. 163–174, 2010.
- 524 [32] C. Boettiger, N. Ross, and A. Hastings, “Early warning signals: the  
525 charted and uncharted territories,” *Theoretical ecology*, vol. 6, no. 3,  
526 pp. 255–264, 2013.
- 527 [33] M. Scheffer, V. Dakos, and E. H. V. Nes, “Slowing down as an early  
528 warning signal for abrupt climate change,” *IOP Conference Series:*  
529 *Earth and Environmental Science*, vol. 105, pp. 14308 – 14312, 2009.

- 530 [34] C. E. Elger and K. Lehnertz, “Seizure prediction by non-linear time  
531 series analysis of brain electrical activity,” *European Journal of Neuro-*  
532 *science*, vol. 10, pp. 786–789, 1998.
- 533 [35] B. Lebaron, “Some relations between volatility and serial correlations in  
534 stock market returns,” *The Journal of Business*, vol. 65, pp. 199–199,  
535 1992.
- 536 [36] S. R. Carpenter and W. A. Brock, “Early warnings of regime shifts in  
537 spatial dynamics using the discrete fourier transform,” *Ecosphere*, vol. 1,  
538 pp. 2150–8925, 2010.
- 539 [37] T. J. Cline, D. A. Seekell, S. R. Carpenter, M. L. Pace, J. R. Hodg-  
540 son, J. F. Kitchell, and B. C. Weidel, “Early warnings of regime shifts:  
541 evaluation of spatial indicators from a whole-ecosystem experiment,”  
542 *Ecosphere*, vol. 5, no. 8, 2014.
- 543 [38] V. Guttal and C. Jayaprakash, “Spatial variance and spatial skewness:  
544 leading indicators of regime shifts in spatial ecological systems,” *Theo-*  
545 *retical Ecology*, vol. 2, no. 1, pp. 3–12, 2009.
- 546 [39] C. R. Wells, E. Y. Klein, and C. T. Bauch, “Policy resistance undermines  
547 superspreader vaccination strategies for influenza,” *PLoS Comput Biol*,  
548 vol. 9, p. e1002945, 03 2013.
- 549 [40] A. Okabe and K. Sugihara, *Spatial analysis along networks: statistical*  
550 *and computational methods*. Wiley, 2012.
- 551 [41] “Spatial correlation at lag 1,” *Early Warning Signals Toolbox*, 2015.
- 552 [42] S. Kefi, V. Guttal, W. A. Brock, S. R. Carpenter, A. M. Ellison, V. N.  
553 Livina, D. A. Seekell, M. Scheffer, E. H. van Nes, and V. Dakos, “Early  
554 warning signals of ecological transitions: Methods for spatial patterns,”  
555 *PLoS ONE*, vol. 9, p. e92097, 03 2014.
- 556 [43] V. Dakos, S. Kefi, M. Rietkerk, E. H. V. Nes, and M. Scheffer, “Slowing  
557 down in spatially patterned ecosystems at the brink of collapse,” *The*  
558 *American Naturalist*, vol. 177, no. 6, 2011.
- 559 [44] C. T. Bauch and D. J. Earn, “Transients and attractors in epidemics,”  
560 *Proceedings of the Royal Society of London B: Biological Sciences*,  
561 vol. 270, no. 1524, pp. 1573–1578, 2003.



- 562 [45] S. Bansal, B. Pourbohloul, and L. A. Meyers, “A comparative analysis  
563 of influenza vaccination programs,” *PLoS Med*, vol. 3, no. 10, p. e387,  
564 2006.
- 565 [46] A. E. Fiore, D. K. Shay, K. Broder, J. K. Iskander, T. M. Uyeki,  
566 G. Mootrey, J. S. Bresee, and N. J. Cox, “Centers for disease control  
567 and prevention,” Aug 2008.
- 568 [47] D. M. Vickers, A. M. Anonychuk, P. De Wals, N. Demartean, and C. T.  
569 Bauch, “Evaluation of serogroup c and acwy meningococcal vaccine pro-  
570 grams: Projected impact on disease burden according to a stochastic  
571 two-strain dynamic model,” *Vaccine*, vol. 33, no. 1, pp. 268–275, 2015.
- 572 [48] P. Erdos and A. Renyi, “On random graphs,” *Publicationes Mathematicae*,  
573 vol. 6, pp. 290–297, 1959.
- 574 [49] R. Albert and A.-L. Barabasi, “On random graphs,” *Science*, vol. 286,  
575 pp. 509–512, 1999.
- 576 [50] D. Easley and J. Kleinberg, *Networks, crowds, and markets reasoning*  
577 *about a highly connected world*. Cambridge University Press, 2010.
- 578 [51] “Synthetic data products for societal infrastructures and proto-  
579 populations: Data set 1.0,”
- 580 [52] D. Ivaneyko, J. Ilnytskyi, B. Berche, and Y. Holovatch, “Local and  
581 cluster critical dynamics of the 3d random-site ising model,” *Physica A:*  
582 *Statistical Mechanics and its Applications*, vol. 370, no. 2, pp. 163–178,  
583 2006.
- 584 [53] J. Dushoff, J. B. Plotkin, S. A. Levin, and D. J. Earn, “Dynamical res-  
585 onance can account for seasonality of influenza epidemics,” *Proceedings*  
586 *of the National Academy of Sciences of the United States of America*,  
587 vol. 101, no. 48, pp. 16915–16916, 2004.
- 588 [54] T. A. e. a. Santibanez, “Flu vaccination coverage, united states, 2014-15  
589 influenza season,” 2015.
- 590 [55] L. D. Elam-Evans, D. Yankey, J. Singleton, and M. Kolasa, “National,  
591 state, and selected local area vaccination coverage among children aged  
592 19-35 months, United States, 2013,” 2014.

- 593 [56] N. Stollenwerk, M. C. Maiden, and V. A. Jansen, “Diversity in  
594 pathogenicity can cause outbreaks of meningococcal disease,” *Proceed-*  
595 *ings of the National Academy of Sciences of the United States of Amer-*  
596 *ica*, vol. 101, no. 27, pp. 10229–10234, 2004.